W-boson mass anomaly and vacuum structure in vector dark matter model with a singlet scalar mediator

Seyed Yaser Ayazi*a and Mojtaba Hosseini†a

^aPhysics Department, Semnan University, P.O. Box. 35131-19111, Semnan, Iran

May 4, 2023

Abstract

Motivated by the deviation of the W boson mass reported by the CDF collaboration, we study an extension of the Standard Model (SM) including a vector dark matter (VDM) candidate and a scalar mediator. In the model, the one-loop corrections induced by the new scalar, shift the W boson mass. We identify the parameter space of the model consistent with dark matter (DM) relic abundance, W mass boson anomaly, invisible Higgs decay at LHC, and direct detection of DM. It is shown that the W-mass anomaly can be explained for the large part of parameter space of VDM mass and scalar mediator mass between $100-124\,\mathrm{GeV}$ by the model. We also investigate the renormalization group equations (RGE) at one-loop order for the model. We show that the contribution of new scalar mediator to RGE, guarantees positivity and vacuum stability of SM Higgs up to Planck scale.

1 Introduction

Recently, CDF-II collaboration published a new result in W boson mass with increased precision $M_{CDF}^{W} = 80.4335 \pm 0.0094$ GeV which deviates from SM prediction by 7σ [1]. The SM prediction for the W boson mass is $M_{SM}^{W} = 80.357 \pm 0.006$ GeV [2]. Needless to say a better understanding of SM calculations, and also more accurate measurements are needed. Nevertheless, a lot of new suggestions have been proposed to explain this anomaly [3–53].

In this paper, we propose a possible explanation of the W boson mass anomaly as well as the nature of dark matter with a extra U(1) dark sector. In [54], the extra U(1) gauge field mix with the U(1) hypercharge via gauge kinetic term, and this kinetic mixing can generate an enhancement of the W boson mass. Another approach for the U(1) extension of SM is to consider an additional scalar field in which the new field can enhance W-boson mass via the loop corrections [55]. In the model, the vector dark field does not mix with the SM gauge field and a scalar field plays the role of mediator between the dark sector and SM. This field shift W-boson mass in loop corrections. We study this simple extension of the SM to explain the W boson mass enhancement and also offer a viable DM candidate with mass ranging from 1 GeV to

^{*}syaser.ayazi@semnan.ac.ir

[†]Mojtabahosseini743@yahoo.com

2 TeV. In the following, we apply various phenomenological constraints such as invisible Higgs decay mode and direct detection experiment in our analysis.

In the context of SM, the vacuum stability and perturbativity have resulted in theoretical bounds on the Higgs mass. The Higgs mass value, together with other relevant parameters such as the top quark mass, affects on the behavior of Higgs potential at very high energy scales, in particular for the sake of electroweak vacuum stability [56], [57]. This is because, for Higgs and top mass values, the Higgs quartic coupling can be very small or even negative. Since the top Yukawa coupling dependency is strong and very subtle, there are different views on an explanation of this issue in literature, some of them favoring [56] and some others disfavoring [58]. In the following, we also ask how the model behaves at a high energy scale and is it computationally reliable? Standard treatment is the study of the running of the coupling constants in terms of the mass scale Λ via the RGE. The three standard problems to consider are the positivity, perturbativity of the coupling constants and the vacuum stability of the model. These issues have been studied in the literature in the presence of a scalar extension of SM [59,60] and it was shown that the vacuum stability requirement can affect the DM relic density. Here, we discuss the requirement of vacuum stability and RGE of the model.

This work is organized as follows: After the introduction, we introduce the model. In section 3, we study conditions of vacuum stability and calculate the RGEs of the model. In section 4, we study the contribution of the model to W-boson mass and probe the consistent parameter space of the model with CDF-II measurement. Invisible Higgs decay constraint on the model study in section. 5. In section. 6, we find the allowed regions in the parameter space which will give rise to the correct DM relic density. We describe combined results consistent with constraints provided and examine the RGEs numerically in section 7. Section 8 contains our conclusions.

2 The Model

In our model, beyond the SM, we employ two new fields to furnish the model: a complex scalar field S which has a unit charge under a dark U(1) gauge symmetry with a dark photon vector field V_{μ} . The model has an additional Z_2 discrete symmetry, under which the vector field V_{μ} and the scalar field transform as follows: $V_{\mu} \to -V_{\mu}$, $S \to S^*$ and all the other fields are even. Z_2 symmetry forbids the kinetic mixing between the vector field V_{μ} and SM $U_Y(1)$ gauge boson B_{μ} , i.e., $V_{\mu\nu}B_{\mu\nu}$. Therefore, the vector field V_{μ} is stable and can be considered a DM candidate. The Lagrangian one can write with assumption is:

$$\mathcal{L} = \mathcal{L}_{SM} + (D'_{\mu}S)^*(D'^{\mu}S) - V(H,S) - \frac{1}{4}V_{\mu\nu}V^{\mu\nu}, \tag{2.1}$$

where \mathcal{L}_{SM} is the SM Lagrangian without the Higgs potential term and

$$D'_{\mu}S = (\partial_{\mu} + ig_{\nu}V_{\mu})S,$$

$$V_{\mu\nu} = \partial_{\mu}V_{\nu} - \partial_{\nu}V_{\mu},$$

and the potential which is renormalizable and invariant under gauge and Z_2 symmetry is:

$$V(H,S) = -\mu_H^2 H^{\dagger} H - \mu_S^2 S^* S + \lambda_H (H^{\dagger} H)^2 + \lambda_S (S^* S)^2 + \lambda_{SH} (S^* S) (H^{\dagger} H).$$
 (2.2)

Note that the quartic portal interaction, $\lambda_{SH}(S^*S)(H^{\dagger}H)$, is the only connection between the dark sector and the SM.

SM Higgs field H, as well as dark scalar S, can receive VEVs breaking respectively the electroweak and $U'_D(1)$ symmetries. In the unitary gauge, the imaginary component of S can be absorbed as the longitudinal component of V_{μ} . In this gauge, we can write

$$H = \frac{1}{\sqrt{2}} \begin{pmatrix} 0 \\ h_1 \end{pmatrix}$$
 and $S = \frac{1}{\sqrt{2}} h_2$, (2.3)

where h_1 and h_2 are real scalar fields which can get VEVs. The tree level potential in unitary gauge is:

$$V_{\text{tree}}(h_1, h_2) = -\frac{1}{2}\mu_H^2 h_1^2 - \frac{1}{2}\mu_S^2 h_2^2 + \frac{1}{4}\lambda_H h_1^4 + \frac{1}{4}\lambda_S h_2^4 + \frac{1}{4}\lambda_{SH} h_1^2 h_2^2.$$
 (2.4)

Given differentiable V_{tree} , one can obtain the Hessian matrix, $\mathcal{H}_{ij}(h_1, h_2) = \frac{\partial^2 V_{\text{tree}}}{\partial h_i \partial h_j}$. In order to get the mass spectrum of the model, it is necessary to consider the sufficient conditions for a local minimum:

$$\left. \frac{\partial V_{\text{tree}}}{\partial h_1} \right|_{h_1 = h_2 = 0} = 0, \tag{2.5}$$

$$\left. \frac{\partial V_{\text{tree}}}{\partial h_2} \right|_{h_1 = h_2 = 0} = 0,\tag{2.6}$$

$$\det \mathcal{H} > 0 \tag{2.7}$$

$$\mathcal{H}_{11} > 0 \tag{2.8}$$

to occur at a point (ν_1, ν_2) . Note that Eq. (2.7) and Eq. (2.8) also imply that $\mathcal{H}_{22} > 0$. Eq. (2.6) leads to

$$\mu_H^2 = \lambda_H \nu_1^2 + \frac{1}{2} \lambda_{SH} \nu_2^2,$$

$$\mu_S^2 = \lambda_S \nu_2^2 + \frac{1}{2} \lambda_{SH} \nu_1^2$$
(2.9)

Eq. (2.9) leads to the non-diagonal mass matrix \mathcal{H} as follows:

$$\mathcal{H}(\nu_1, \nu_2) = \begin{pmatrix} 2\lambda_H \nu_1^2 & \lambda_{SH} \nu_1 \nu_2 \\ \lambda_{SH} \nu_1 \nu_2 & 2\lambda_S \nu_2^2 \end{pmatrix}$$
 (2.10)

Therefore, according to the conditions $\mathcal{H}_{11} > 0$ and $\mathcal{H}_{22} > 0$ and Eq. (2.7) we should have

$$\lambda_H > 0 \ , \ \lambda_S > 0 \ , \ \lambda_{SH}^2 < 4\lambda_H \lambda_S$$
 (2.11)

Now by substituting $h_1 \to \nu_1 + h_1$ and $h_2 \to \nu_2 + h_2$, the fields h_1 and h_1 mix with each other and they can be rewritten by the mass eigenstates H_1 and H_1 as

$$\begin{pmatrix} h_1 \\ h_2 \end{pmatrix} = \begin{pmatrix} \cos\alpha & \sin\alpha \\ -\sin\alpha & \cos\alpha \end{pmatrix} \begin{pmatrix} H_1 \\ H_2 \end{pmatrix}, \tag{2.12}$$

where α is the mixing angle. After symmetry breaking, we have

$$\nu_{2} = \frac{M_{V}}{g_{v}}, \qquad \sin \alpha = \frac{\nu_{1}}{\sqrt{\nu_{1}^{2} + \nu_{2}^{2}}}$$

$$\lambda_{H} = \frac{\cos^{2} \alpha M_{H_{1}}^{2} + \sin^{2} \alpha M_{H_{2}}^{2}}{2\nu_{1}^{2}}$$

$$\lambda_{S} = \frac{\sin^{2} \alpha M_{H_{1}}^{2} + \cos^{2} \alpha M_{H_{2}}^{2}}{2\nu_{2}^{2}}$$

$$\lambda_{SH} = \frac{\left(M_{H_{2}}^{2} - M_{H_{1}}^{2}\right) \sin \alpha \cos \alpha}{\nu_{1}\nu_{2}}$$
(2.13)

Since U(1) gauge symmetries of two sectors are only broken spontaneously, gauge bosons from the two sectors will not mix at any order of perturbation theory and the field renormalisation constants are defined independently in each sector [61]. This means vector dark matter still is stable and DM candidate.

The mass eigenstates of scalar fields can be written as following:

$$M_{H_2,H_1}^2 = \lambda_H \nu_1^2 + \lambda_S \nu_2^2 \pm \sqrt{(\lambda_H \nu_1^2 - \lambda_S \nu_2^2)^2 + \lambda_{SH}^2 \nu_1^2 \nu_2^2},$$
 (2.14)

where we take $M_{H_1} = 125$ GeV and $\nu_1 = 246$ GeV. Note that, beside of SM parameters, the model has only three free parameters g_v , M_{H_2} and M_V .

3 Vacuum stability and RGE

A prominent feature of the study of high energy physics is the evolution of the coupling constants with energy. This has become an incentive to further strengthen theories such as the GUT and supersymmetry by merging couplings at high energies [62]. Renormalization Group Equation(RGE) describes the behavior of quantities with energy. After the discovery of the Higgs particle by ATLAS and CMS experiments at the LHC in 2012, the vacuum stability study has been done more clearly [55, 59, 60, 63–65]. In the SM, the Higgs quartic coupling becomes negative at the scale 10^{10} GeV, and the Higgs non-zero VEV is no longer a minimum of the theory. The reason for this is that the top quark has a large negative contribution to the RGE for λ_H . We will show the running of λ_H in SM in the next sections.

There are three types of theoretical constraints on the couplings in the model. The first is the perturbative unitarity condition of the couplings, which includes the following relations [66]:

$$|\lambda_S| < 4\pi$$
 , $|\lambda_H| < 4\pi$, $|\lambda_{SH}| < 8\pi$, $3\lambda_H + 2\lambda_S + \sqrt{(3\lambda_H - 2\lambda_S)^2 + 2\lambda_{SH}^2} < 8\pi$, $|g_v| < \sqrt{4\pi}$ (3.1)

and the second is vacuum stability of the model dictates some other constraints on the couplings such that for self-coupling constants. In this regard, we should have λ_i and $\lambda_H > 0$. On the other hand, by adding a new scalar mediator the vacuum structure of the model will be modified. The third condition is positivity where potential must be well-defined and positive at all scales. The requirement of positivity for the potential implies the following relations:

$$\lambda_H > 0, \lambda_S > 0, \lambda_{SH} > -2\sqrt{\lambda_H \lambda_S} \tag{3.2}$$

Also, the common investigation for vacuum stability analyses in the literature begins with the RGE improved potential and choice of the renormalization scale to minimize the one-loop potential. In this light, we consider the running of the coupling constants with energy. The Model is implemented in SARAH [67] to compute β functions and their runnings. We calculate the one-loop RGE and one-loop β functions for scalar couplings and dark coupling including the following relationships:

$$(16\pi^{2})\beta_{\lambda_{S}} = -20\lambda_{S}^{2} - 2\lambda_{SH}^{2} - 6g_{v}^{4} - 12g_{v}^{2}\lambda_{S},$$

$$(16\pi^{2})\beta_{\lambda_{SH}} = -\frac{3}{2}g_{1}^{2}\lambda_{SH} - \frac{9}{2}g_{2}^{2}\lambda_{SH} - 12\lambda_{SH}\lambda_{H} - 8\lambda_{SH}\lambda_{S} - 4\lambda_{SH}^{2} + 6\lambda_{SH}\lambda_{t}^{2} - 6g_{v}^{2}\lambda_{SH},$$

$$(16\pi^{2})\beta_{\lambda_{H}} = -\frac{3}{8}g_{1}^{4} - \frac{3}{4}g_{1}^{2}g_{2}^{2} - \frac{9}{8}g_{2}^{4} - 3g_{1}^{2}\lambda_{H} - 9g_{2}^{2}\lambda_{H} - 24\lambda_{H}^{2} - \lambda_{SH}^{2} + 12\lambda_{H}\lambda_{t}^{2} + 6\lambda_{t}^{4},$$

$$(16\pi^{2})\beta_{g_{v}} = \frac{1}{3}g_{v}^{3}.$$

$$(3.3)$$

where λ_t is top Yukawa coupling and $\beta_a \equiv \mu \frac{da}{d\mu}$ that μ is the renormalization scale with initial value $\mu_0 = 100$ GeV. The β functions of couplings, g_1 , g_2 and g_3 are given to one-loop order by:

$$(16\pi^2)\beta_{g_1} = \frac{41}{6}g_1^3,$$

$$(16\pi^2)\beta_{g_2} = -\frac{19}{6}g_2^3,$$

$$(16\pi^2)\beta_{g_3} = -7g_3^3.$$
(3.4)

Among the Yukawa couplings of SM, the top quark has the largest contribution compared with other fermions in the SM. Therefore, we set all the SM Yukawa couplings equal to zero and consider only the top quark coupling. The RGE of top quark Yukawa coupling is given to one-loop order by

$$(16\pi^2)\beta_{\lambda_t} = -\frac{17}{12}g_1^2\lambda_t - \frac{9}{4}g_2^2\lambda_t - 8g_3^2\lambda_t + \frac{9}{2}\lambda_t^3.$$
(3.5)

In the following, we first study experimental constraints on the model, and then in the final section, we investigate conditions of the Higgs stability and RGE of coupling parameters of the model.

4 W-Mass Anomaly

To explain the CDF-II anomaly, we study W-mass correction in the context of the model. The corrections of new physics to the W-boson mass can be written in terms of the Peskin-Takeuchi oblique parameters S, T, and U. The Peskin-Takeuchi parameters are only sensitive to new physics that contribute to the oblique corrections, i.e., the vacuum polarization corrections to four-fermion scattering processes. In general, the SM contribution to an oblique parameter is subtracted from the new physics contribution to define the oblique parameter. The effects of S, T, and U on W boson mass can be expressed as follows [68]:

$$\Delta M_W^2 = \frac{M_{SM}^2}{c_W^2 - s_W^2} \left(-\frac{\alpha S}{2} + c_W^2 \alpha T + \frac{c_W^2 - s_W^2}{4s_W^2} \alpha U \right). \tag{4.1}$$

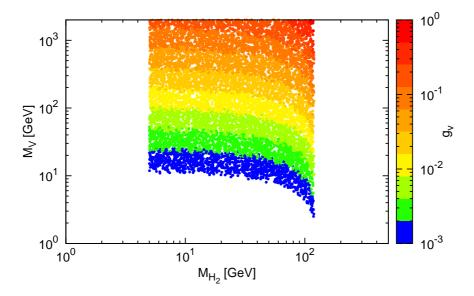


Figure 1: Scatter points depict allowed range of parameters space of the model consistent with W-boson mass measurement.

where M_{SM} is SM of W-boson mass, c_W and s_W are cosine and sine of Weinberg angle. Oblique parameters S, T, and U for our model are as follows [69]:

$$\alpha S = \frac{g^2 \sin^2 \alpha}{96\pi^2} [(\ln M_{H_2}^2 + G(M_{H_2}^2, M_Z^2)) - (\ln M_{H_1}^2 + G(M_{H_1}^2, M_Z^2))], \tag{4.2}$$

$$\alpha T = \frac{3g^2 sin^2 \alpha}{64\pi^2 s_W^2 M_W^2} [(F(M_Z^2, M_{H_2}^2) - F(M_W^2, M_{H_2}^2)) - (F(M_Z^2, M_{H_1}^2) - F(M_W^2, M_{H_1}^2))], \quad (4.3)$$

$$\alpha U = \frac{g^2 \sin^2 \alpha}{96\pi^2} [(G(M_{H_2}^2, M_W^2) - G(M_{H_2}^2, M_Z^2)) - (G(M_{H_1}^2, M_W^2) - G(M_{H_1}^2, M_Z^2))], \tag{4.4}$$

where

$$g^2 = 4\pi\alpha_{QED} \tag{4.5}$$

$$F(x,y) = \begin{cases} \frac{x+y}{2} - \frac{xy}{x-y} ln\frac{x}{y} & for \ x \neq y, \\ 0 & for \ x = y, \end{cases}$$
(4.6)

$$G(x,y) = -\frac{79}{3} + 9\frac{x}{y} - 2\frac{x^2}{y^2} + (-10 + 18\frac{x}{y} - 6\frac{x^2}{y^2} + \frac{x^3}{y^3} - 9\frac{x+y}{x-y})ln\frac{x}{y} + (12 - 4\frac{x}{y} + \frac{x^2}{y^2})\frac{f(x,x^2 - 4xy)}{y},$$

$$(4.7)$$

$$f(a,b) = \begin{cases} \sqrt{bln} \left| \frac{a - \sqrt{b}}{a + \sqrt{b}} \right| & \text{for } b > 0 \\ 0 & \text{for } b = 0 \\ 2\sqrt{-b} Arctan \frac{\sqrt{-b}}{a} & \text{for } b < 0. \end{cases}$$

$$(4.8)$$

We know that in the model U(1) dark gauge symmetry have been broken spontaneously and Z_2 still is symmetry of the model and so there is no mixing between SM and dark gauge bosons [61]. Meanwhile, as it is clear from the above relations extra gauged U(1) symmetry does not contribute to W- mass anomaly and contributions are the same as those found in the analysis

of the plain Higgs portal [55]. but, contributions of parameters M_V and g_v appear in the form of $\sin \alpha$ in the formulas of (4.2), (4.3) and (4.4). To study the model parameter space, other than theoretical constraints (such as perturbativity condition and vacuum stability), it is necessary to consider the experimental upper limit on mixing angle α . For low masses, $M_{H_2} < 5$ GeV, the strongest limit comes from decay $B \to K\ell\ell$ [70, 71]. It was shown that for this range of parameters, $\sin \alpha$ should be smaller than 10^{-3} . Between 5-12 GeV, the constraint on $\sin \alpha < 0.5$ is imposed by the decay of a low-mass Higgs boson in radiative decay of the Y and the DELPHI searches for a light Higgs in Z-decay [72,73]. For above this mass range to about 65 GeV, an overall result of the Higgs signal strength measured by ATLAS and CMS [74] severely constrains the mixing angle to values smaller than $sin\alpha < 0.12$. For the larger values of M_{H_2} , the lower limit is set by the LHC constraints on the mixing angle in which $sin\alpha \leq 0.44$ [75, 76]. In the following, for low mass M_{H_2} in which decay of SM Higgs like to H_2 is kinematically possible, we consider severe upper limit on mixing angle and for large M_{H_2} mass, we relax this bound. As was discussed in the previous section, the present model has three free parameters, g_v , M_{H_2} and M_V . In addition to the mixing angle constraints, we also make the following choices for the mass parameters:

- The DM mass M_V is between 1-2000 GeV;
- The mediator scalar mass (M_{H_2}) is between 1-500 GeV;

We scan over the three-dimensional parameters g_v , M_{H_2} , and M_V to probe a consistent range of parameters space with observables. In figure. 1, we depict the allowed range of parameters of the model which is consistent with CDF measurement for W-boson mass. Note that, for a large value of M_{H_2} , we choose $sin\alpha \leq 0.44$ on the mixing angle, and for $M_{H_2} < 65$ GeV, we suppose $\alpha < 6.9$ ° to satisfy ATLAS and CMS upper limit on the mixing angle. As is seen in the figure, the W-Mass measurement, for $M_{H_2} \lesssim 4.5$ GeV and $M_{H_2} \gtrsim 124$ GeV, excludes the parameters space of the model. However, for M_{H_2} between 4.5-124 GeV and M_V between 1-2000 GeV, the model is consistent with the W-mass anomaly.

5 Invisible Higgs decay

In the model, SM Higgs-like can decay invisibly into a pair of DM if kinematically allowed. Also, it can decay to another Higgs boson for $M_{H_2} < 1/2M_{H_1}$. Therefore, H_1 can contribute to the invisible decay mode with a branching ratio:

$$Br(H_1 \to \text{Invisible}) = \frac{\Gamma(H_1 \to 2VDM) + \Gamma(H_1 \to 2H_2)}{\Gamma(h)_{SM} + \Gamma(H_1 \to 2VDM) + \Gamma(H_1 \to 2H_2)},$$
 (5.1)

where $\Gamma(h)_{SM}=4.15$ [MeV] is total width of Higgs boson [77]. The partial width for processes $H_1 \to 2VDM$ and $H_1 \to 2H_2$ are given by:

$$\Gamma(H_1 \to 2VDM) = \frac{g_v^4 v_2^2 \sin^2 \alpha}{8\pi M_{H_1}} \sqrt{1 - \frac{4M_V^2}{M_{H_1}^2}}.$$
 (5.2)

$$\Gamma(H_1 \to 2H_2) = \frac{a^2}{8\pi M_{H_1}} \sqrt{1 - \frac{4M_{H_2}^2}{M_{H_1}^2}}.$$
 (5.3)

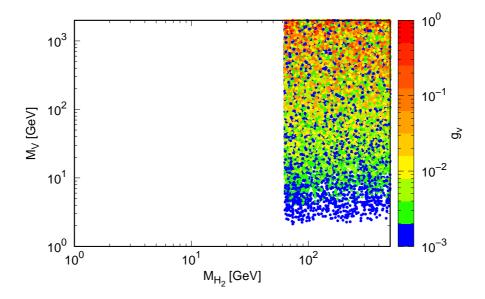


Figure 2: The cross points depict allowed region which is consistent with invisible Higgs decay at [82].

where $a = (1/2\cos^3\alpha - \sin^2\alpha\cos\alpha)v_1$. The SM prediction for the branching ratio of the Higgs boson decaying to invisible particles which coming from process $h \to ZZ^* \to 4\nu$ [78], [79], [80], [81] is, 1.2×10^{-3} . CMS Collaboration has reported the observed (expected) upper limit on the invisible branching fraction of the Higgs boson to be 0.18(0.10) at the 95% confidence level, by assuming the SM production cross section [82]. A Similar analysis was performed by ATLAS collaboration in which an observed upper limit of 0.145 is placed on the branching fraction of its decay into invisible particles at a 95% confidence level [83].

Figure. 2, shows the allowed range of parameters by considering CMS [82] upper limit for invisible Higgs mode. In this figure, we consider LHC bound on the mixing angle $\sin \alpha < 0.12$. For $M_{H_2} < 1/2M_{SM}$ CMS upper limit excludes the parameters space. Note that this upper limit practically can not constraint the model for low mass DM and also part of the parameters space in which invisible Higgs decay is forbidden.

6 Relic Density

The evolution of the number density of DM particles (n_X) with time is governed by the Boltzmann equation:

$$\dot{n}_X + 3Hn_X = -\langle \sigma_{ann} \nu_{rel} \rangle [n_X^2 - (n_X^{eq})^2], \tag{6.1}$$

where H is the Hubble parameter and $n_X^{eq} \sim (m_X T)^{3/2} e^{-m_X/T}$ is the particle density before particles get out of equilibrium. The dominant Feynman diagrams for dark matter production processes are shown in the Fig .3. In this regard, we calculate the relic density numerically for the VDM particle by implementing the model into micrOMEGAs [84]. We investigate viable parameter space which satisfies constraints from observed DM relic density (according to the

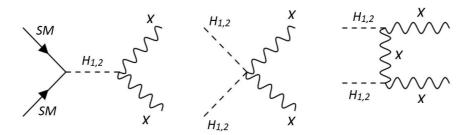


Figure 3: The dominant Feynman diagrams for dark matter relic density production cross section.

data of Planck collaboration [85]):

$$\Omega_{DM}h^2 = 0.1199 \pm 0.0027. \tag{6.2}$$

The allowed range of parameter space corresponding to this constraint is depicted in figure 4. As seen in the figure, for small values of VDM mass ($M_V \lesssim 22 \text{ GeV}$), relic density measurement excludes the model for $10^{-3} \leqslant g_v \leqslant 1$. This issue arises from the fact that we have chosen g_v coupling larger than 10^{-3} . For smaller values of g_v , the model satisfy relic density constraint.

7 Final Results

Before, we present a combined analysis of all constraints, let us turn our attention to the direct detection (DD) of VDM in the model. At the tree level, a VDM particle can interact elastically with a nucleon either through H_1 or via H_2 exchange [86,87]. Presently, the XENON1T experiment [88] excludes new parameter space for the WIMP-nucleon spin-independent elastic scatter cross-section above 6 GeV with a minimum of $4.1 \times 10^{-47} cm^2$ at 30 GeV. We restrict the model with these results. Figure 5 shows the parameter space of the model in agreement with the direct detection and relic density constraints. In addition, in this figure we have also used the results of the LUX-ZEPLIN(LZ) experiment [89] that was published recently.

The direct detection restrictions and constraints discussed in the previous sections are summarized in figure. 6. The cross points show allowed region consistent with relic density, W-mass anomaly, direct detection as well as the invisible decay rate.

The outcome of imposing these experimental constraints on the model is for a large portion of VDM mass values, narrow region of scalar mediator H_2 (100 GeV $\lesssim M_{\rm H_2} \lesssim 124$ GeV), and $0 < g_v \leqslant 1$ all observational constraints are satisfied. The point is that for M_{H_2} and

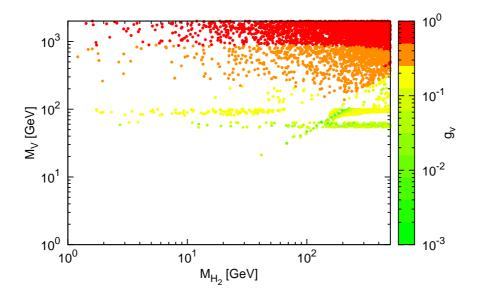


Figure 4: The allowed range of parameter space consistent with DM relic density.

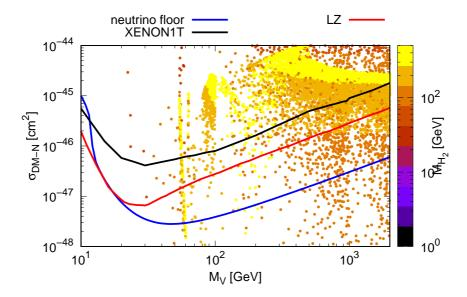


Figure 5: The allowed range of parameter space consistent with DM relic density and DD.

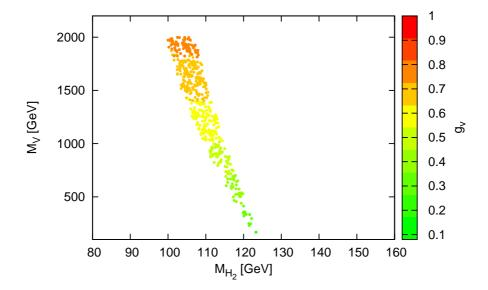


Figure 6: Final results for allowed ranges of parameters of the model. The cross points depict allowed region which is consistent with relic density, direct detection, W mass anomaly and invisible decay rate.

 $M_V < 1/2M_{SM}$ (in which H_1 can decay to H_2 and VDM), and $M_{H_2} > 124$ GeV the model is respectively excluded by invisible Higgs upper limit and W-mass CDF-II measurement.

In section. 3, we analyze RGEs of coupling of the model. We show that adding a new VDM and scalar mediator, the RGEs will be modified. It is interesting to see behavior of RGEs of couplings in Planck scale. We solve the RG equations numerically and determine the RG evolution of the couplings of the models. For input parameters, we pick benchmark points for parameters of the model that are consistent with all constraints considered previously in the paper. Similar analyses with different input parameters have been performed for U(1) extension of SM in Ref [55]. The running of couplings up to the Planck scale have been shown in Figures.(7 .a-c). In Figure. (7 .d), we compared running of λ_H in the model with SM Higgs coupling. As it is known, SM Higgs coupling will be negative for $\mu > 10^{10}$ GeV. This means, it is not possible to establish all three conditions (perturbativity, vacuum stability and positivity) simultaneously in any scale. It is remarkable that the SM stability problem (positivity of λ_H) is solved in the model. This issue arises that λ_{SH} changes very little in our model. This leads small changes for λ_H and as a result, λ_H remains positive until the Planck scale.

8 Conclusions

We proposed a model to explain the W boson mass anomaly reported by the CDF-II collaboration. We studied an U(1) extension of the SM including a VDM candidate and a scalar mediator. In the model, there is no kinetic mixing between the VDM field and SM Z-boson, but scalar field exchange between SM and dark side. To explain the W mass anomaly one needs

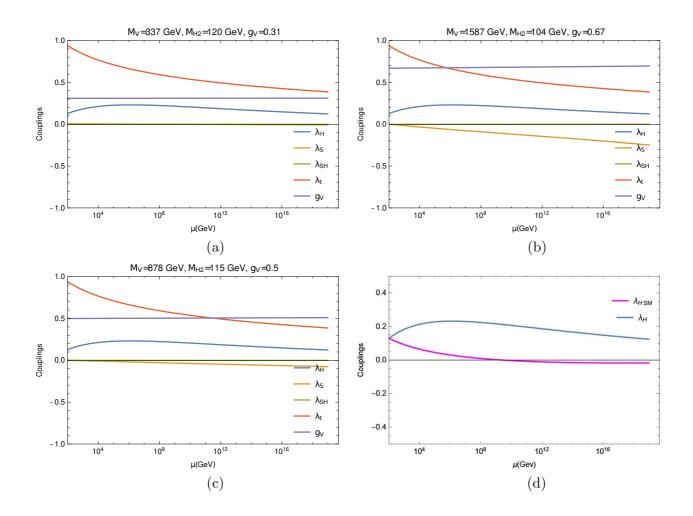


Figure 7: Running of couplings of the model up to Planck scale. We select sample point in which all the experimental constraints considered in the paper are satisfied.

extra degrees of freedom that affects on W-boson mass. In the model, the one-loop corrections induced by the new scalar can shift the W boson mass. We have also imposed constraints on the Higgs mixing angle and other parameters of the model by investigating of relic density of DM, invisible Higgs decay mode at LHC and direct detection of DM. We have shown that the model for a large part of VDM mass values, scalar mediator mass range 100 GeV \lesssim $M_{\rm H_2} \lesssim$ 124 GeV and $0 < g_v \leqslant 1$ can explain W-mass anomaly and satisfy all experimental constraints.

We have also investigated the effects and consequences of the RGE at one-loop order on the model. It was shown that adding of new fields to SM, changes positivity and stability conditions of SM Higgs as it will be stable up to Planck scale.

Acknowledgments

We would like to thank Dr. Ahmad Mohamadnejad for helping with micrOMEGAs code issues.

References

- [1] CDF collaboration, High-precision measurement of the W boson mass with the CDF II detector, Science 376 (2022) 170.
- [2] Particle Data Group collaboration, Review of Particle Physics, PTEP 2020 (2020) 083C01.
- [3] K. Ghorbani and P. Ghorbani, W-Boson Mass Anomaly from Scale Invariant 2HDM, 2204.09001.
- [4] Y. Cheng, X.-G. He, F. Huang, J. Sun and Z.-P. Xing, Dark photon kinetic mixing effects for CDF W mass excess, 2204.10156.
- [5] D. Borah, S. Mahapatra and N. Sahu, Singlet-doublet fermion origin of dark matter, neutrino mass and W-mass anomaly, Phys. Lett. B 831 (2022) 137196 [2204.09671].
- [6] G. Arcadi and A. Djouadi, The 2HD+a model for a combined explanation of the possible excesses in the CDF $\mathbf{M}_{\mathbf{W}}$ measurement and $(\mathbf{g} \mathbf{2})_{\mu}$ with Dark Matter, 2204.08406.
- [7] K. I. Nagao, T. Nomura and H. Okada, A model explaining the new CDF II W boson mass linking to muon g-2 and dark matter, 2204.07411.
- [8] J. Kawamura, S. Okawa and Y. Omura, W boson mass and muon g-2 in a lepton portal dark matter model, 2204.07022.
- [9] Y.-Z. Fan, T.-P. Tang, Y.-L. S. Tsai and L. Wu, Inert Higgs Dark Matter for New CDF W-boson Mass and Detection Prospects, 2204.03693.
- [10] C.-T. Lu, L. Wu, Y. Wu and B. Zhu, Electroweak Precision Fit and New Physics in light of W Boson Mass, 2204.03796.

- [11] P. Athron, A. Fowlie, C.-T. Lu, L. Wu, Y. Wu and B. Zhu, The W boson Mass and Muon g-2: Hadronic Uncertainties or New Physics?, 2204.03996.
- [12] G.-W. Yuan, L. Zu, L. Feng, Y.-F. Cai and Y.-Z. Fan, Hint on new physics from the W-boson mass excess—axion-like particle, dark photon or Chameleon dark energy, 2204.04183.
- [13] A. Strumia, Interpreting electroweak precision data including the W-mass CDF anomaly, 2204.04191.
- [14] J. M. Yang and Y. Zhang, Low energy SUSY confronted with new measurements of W-boson mass and muon q-2, 2204.04202.
- [15] J. de Blas, M. Pierini, L. Reina and L. Silvestrini, Impact of the recent measurements of the top-quark and W-boson masses on electroweak precision fits, 2204.04204.
- [16] X. K. Du, Z. Li, F. Wang and Y. K. Zhang, Explaining The Muon g-2 Anomaly and New CDF II W-Boson Mass in the Framework of (Extra)Ordinary Gauge Mediation, 2204.04286.
- [17] T.-P. Tang, M. Abdughani, L. Feng, Y.-L. S. Tsai, J. Wu and Y.-Z. Fan, NMSSM neutralino dark matter for W-boson mass and muon g-2 and the promising prospect of direct detection, 2204.04356.
- [18] G. Cacciapaglia and F. Sannino, The W boson mass weighs in on the non-standard Higgs, Phys. Lett. B 832 (2022) 137232 [2204.04514].
- [19] M. Blennow, P. Coloma, E. Fernández-Martínez and M. González-López, *Right-handed neutrinos and the CDF II anomaly*, 2204.04559.
- [20] K. Sakurai, F. Takahashi and W. Yin, Singlet extensions and W boson mass in the light of the CDF II result, 2204.04770.
- [21] J. Fan, L. Li, T. Liu and K.-F. Lyu, W-Boson Mass, Electroweak Precision Tests and SMEFT, 2204.04805.
- [22] X. Liu, S.-Y. Guo, B. Zhu and Y. Li, Correlating gravitational waves with W-boson mass, FIMP dark matter, and majorana seesaw mechanism, 2204.04834.
- [23] H. M. Lee and K. Yamashita, A Model of Vector-like Leptons for the Muon g-2 and the W Boson Mass, 2204.05024.
- [24] E. Bagnaschi, J. Ellis, M. Madigan, K. Mimasu, V. Sanz and T. You, SMEFT Analysis of m_W , 2204.05260.
- [25] A. Paul and M. Valli, Violation of custodial symmetry from W-boson mass measurements, 2204.05267.

- [26] H. Bahl, J. Braathen and G. Weiglein, New physics effects on the W-boson mass from a doublet extension of the SM Higgs sector, 2204.05269.
- [27] P. Asadi, C. Cesarotti, K. Fraser, S. Homiller and A. Parikh, Oblique Lessons from the W Mass Measurement at CDF II, 2204.05283.
- [28] L. Di Luzio, R. Gröber and P. Paradisi, Higgs physics confronts the MW anomaly, Phys. Lett. B 832 (2022) 137250 [2204.05284].
- [29] P. Athron, M. Bach, D. H. J. Jacob, W. Kotlarski, D. Stöckinger and A. Voigt, Precise calculation of the W boson pole mass beyond the Standard Model with FlexibleSUSY, 2204.05285.
- [30] J. Gu, Z. Liu, T. Ma and J. Shu, Speculations on the W-Mass Measurement at CDF, 2204.05296.
- [31] K. S. Babu, S. Jana and V. P. K., Correlating W-Boson Mass Shift with Muon g-2 in the 2HDM, 2204.05303.
- [32] Y. Heo, D.-W. Jung and J. S. Lee, Impact of the CDF W-mass anomaly on two Higgs doublet model, 2204.05728.
- [33] X. K. Du, Z. Li, F. Wang and Y. K. Zhang, Explaining The New CDF II W-Boson Mass Data In The Georgi-Machacek Extension Models, 2204.05760.
- [34] K. Cheung, W.-Y. Keung and P.-Y. Tseng, Iso-doublet Vector Leptoquark solution to the Muon g-2, R_{K,K^*} , R_{D,D^*} , and W-mass Anomalies, 2204.05942.
- [35] A. Crivellin, M. Kirk, T. Kitahara and F. Mescia, Correlating $t \to cZ$ to the W Mass and B Physics with Vector-Like Quarks, 2204.05962.
- [36] M. Endo and S. Mishima, New physics interpretation of W-boson mass anomaly, 2204.05965.
- [37] T. Biekötter, S. Heinemeyer and G. Weiglein, Excesses in the low-mass Higgs-boson search and the W-boson mass measurement, 2204.05975.
- [38] R. Balkin, E. Madge, T. Menzo, G. Perez, Y. Soreq and J. Zupan, On the implications of positive W mass shift, JHEP 05 (2022) 133 [2204.05992].
- [39] X.-F. Han, F. Wang, L. Wang, J. M. Yang and Y. Zhang, A joint explanation of W-mass and muon g-2 in 2HDM, 2204.06505.
- [40] Y. H. Ahn, S. K. Kang and R. Ramos, Implications of New CDF-II W Boson Mass on Two Higgs Doublet Model, 2204.06485.
- [41] M.-D. Zheng, F.-Z. Chen and H.-H. Zhang, The Wℓν-vertex corrections to W-boson mass in the R-parity violating MSSM, 2204.06541.

- [42] A. Ghoshal, N. Okada, S. Okada, D. Raut, Q. Shafi and A. Thapa, Type III seesaw with R-parity violation in light of m_W (CDF), 2204.07138.
- [43] P. Fileviez Perez, H. H. Patel and A. D. Plascencia, On the W-mass and New Higgs Bosons, 2204.07144.
- [44] P. Mondal, Enhancement of the **W** boson mass in the Georgi-Machacek model, 2204.07844.
- [45] D. Borah, S. Mahapatra, D. Nanda and N. Sahu, Type II Dirac Seesaw with Observable ΔN_{eff} in the light of W-mass Anomaly, 2204.08266.
- [46] T. A. Chowdhury, J. Heeck, S. Saad and A. Thapa, W boson mass shift and muon magnetic moment in the Zee model, 2204.08390.
- [47] A. Bhaskar, A. A. Madathil, T. Mandal and S. Mitra, Combined explanation of W-mass, muon g-2, $R_{K^{(*)}}$ and $R_{D^{(*)}}$ anomalies in a singlet-triplet scalar leptoquark model, 2204.09031.
- [48] G. Lazarides, R. Maji, R. Roshan and Q. Shafi, Heavier W-boson, dark matter and gravitational waves from strings in an SO(10) axion model, 2205.04824.
- [49] G. Senjanović and M. Zantedeschi, SU(5) grand unification and W-boson mass, 2205.05022.
- [50] T. A. Chowdhury and S. Saad, Leptoquark-vectorlike quark model for m_W (CDF), $(g-2)_{\mu}$, $R_{K^{(*)}}$ anomalies and neutrino mass, 2205.03917.
- [51] J. J. Heckman, Extra W-Boson Mass from a D3-Brane, 2204.05302.
- [52] J. Cao, L. Meng, L. Shang, S. Wang and B. Yang, Interpreting the W mass anomaly in the vectorlike quark models, 2204.09477.
- [53] Q. Zhou and X.-F. Han, The CDF W-mass, muon g-2, and dark matter in a $U(1)_{L_{\mu}-L_{\tau}}$ model with vector-like leptons, 2204.13027.
- [54] K.-Y. Zhang and W.-Z. Feng, Explaining W boson mass anomaly and dark matter with a U(1) dark sector, 2204.08067.
- [55] M. Duch, B. Grzadkowski and M. McGarrie, A stable Higgs portal with vector dark matter, JHEP **09** (2015) 162 [1506.08805].
- [56] F. Bezrukov, M. Y. Kalmykov, B. A. Kniehl and M. Shaposhnikov, Higgs Boson Mass and New Physics, JHEP 10 (2012) 140 [1205.2893].
- [57] D. Buttazzo, G. Degrassi, P. P. Giardino, G. F. Giudice, F. Sala, A. Salvio et al., Investigating the near-criticality of the Higgs boson, JHEP 12 (2013) 089 [1307.3536].

- [58] G. Degrassi, S. Di Vita, J. Elias-Miro, J. R. Espinosa, G. F. Giudice, G. Isidori et al., Higgs mass and vacuum stability in the Standard Model at NNLO, JHEP 08 (2012) 098 [1205.6497].
- [59] K. Ghorbani, Renormalization group equation analysis of a pseudoscalar portal dark matter model, J. Phys. G 44 (2017) 105006 [1702.08711].
- [60] M. Gonderinger, H. Lim and M. J. Ramsey-Musolf, Complex Scalar Singlet Dark Matter: Vacuum Stability and Phenomenology, Phys. Rev. D 86 (2012) 043511 [1202.1316].
- [61] S. Glaus, M. Mühlleitner, J. Müller, S. Patel and R. Santos, Electroweak Corrections to Dark Matter Direct Detection in a Vector Dark Matter Model, JHEP 10 (2019) 152 [1908.09249].
- [62] A. Wulzer, Behind the Standard Model, in 2015 European School of High-Energy Physics, 1, 2019, 1901.01017.
- [63] A. Abada and S. Nasri, Renormalization group equations of a cold dark matter two-singlet model, Phys. Rev. D 88 (2013) 016006 [1304.3917].
- [64] S. Baek, P. Ko, W.-I. Park and E. Senaha, Vacuum structure and stability of a singlet fermion dark matter model with a singlet scalar messenger, JHEP 11 (2012) 116 [1209.4163].
- [65] P. Ghorbani, Vacuum stability vs. positivity in real singlet scalar extension of the standard model, Nucl. Phys. B 971 (2021) 115533 [2104.09542].
- [66] K. Hashino, M. Kakizaki, S. Kanemura, P. Ko and T. Matsui, Gravitational waves from first order electroweak phase transition in models with the U(1)_X gauge symmetry, JHEP 06 (2018) 088 [1802.02947].
- [67] F. Staub, Exploring new models in all detail with SARAH, Adv. High Energy Phys. 2015 (2015) 840780 [1503.04200].
- [68] M. E. Peskin and T. Takeuchi, Estimation of oblique electroweak corrections, Phys. Rev. D 46 (1992) 381.
- [69] W. Grimus, L. Lavoura, O. M. Ogreid and P. Osland, The Oblique parameters in multi-Higgs-doublet models, Nucl. Phys. B 801 (2008) 81 [0802.4353].
- [70] LHCB collaboration, Differential branching fraction and angular analysis of the $B^+ \to K^+ \mu^+ \mu^-$ decay, JHEP **02** (2013) 105 [1209.4284].
- [71] Belle collaboration, Measurement of the Differential Branching Fraction and Forward-Backward Asymmetry for $B \to K^{(*)} \ell^+ \ell^-$, Phys. Rev. Lett. **103** (2009) 171801 [0904.0770].
- [72] DELPHI collaboration, Search for low mass Higgs bosons produced in Z0 decays, Z. Phys. C 51 (1991) 25.

- [73] BABAR collaboration, Search for di-muon decays of a low-mass Higgs boson in radiative decays of the Υ(1S), Phys. Rev. D 87 (2013) 031102 [1210.0287].
- [74] ATLAS, CMS collaboration, Measurements of the Higgs boson production and decay rates and constraints on its couplings from a combined ATLAS and CMS analysis of the LHC pp collision data at $\sqrt{s} = 7$ and 8 TeV, JHEP **08** (2016) 045 [1606.02266].
- [75] A. Farzinnia, H.-J. He and J. Ren, Natural Electroweak Symmetry Breaking from Scale Invariant Higgs Mechanism, Phys. Lett. B 727 (2013) 141 [1308.0295].
- [76] A. Farzinnia and J. Ren, Higgs Partner Searches and Dark Matter Phenomenology in a Classically Scale Invariant Higgs Boson Sector, Phys. Rev. D 90 (2014) 015019 [1405.0498].
- [77] LHC HIGGS CROSS SECTION WORKING GROUP collaboration, Handbook of LHC Higgs Cross Sections: 1. Inclusive Observables, 1101.0593.
- [78] A. Denner, S. Heinemeyer, I. Puljak, D. Rebuzzi and M. Spira, Standard Model Higgs-Boson Branching Ratios with Uncertainties, Eur. Phys. J. C 71 (2011) 1753 [1107.5909].
- [79] S. Dittmaier et al., Handbook of LHC Higgs Cross Sections: 2. Differential Distributions, 1201.3084.
- [80] O. Brein, A. Djouadi and R. Harlander, NNLO QCD corrections to the Higgs-strahlung processes at hadron colliders, Phys. Lett. B 579 (2004) 149 [hep-ph/0307206].
- [81] LHC HIGGS CROSS SECTION WORKING GROUP collaboration, Handbook of LHC Higgs Cross Sections: 3. Higgs Properties, 1307.1347.
- [82] CMS collaboration, Search for invisible decays of the Higgs boson produced via vector boson fusion in proton-proton collisions at $\sqrt{s} = 13$ TeV, 2201.11585.
- [83] ATLAS collaboration, Search for invisible Higgs-boson decays in events with vector-boson fusion signatures using 139 fb⁻¹ of proton-proton data recorded by the ATLAS experiment, 2202.07953.
- [84] G. Bélanger, F. Boudjema, A. Pukhov and A. Semenov, micrOMEGAs4.1: two dark matter candidates, Comput. Phys. Commun. 192 (2015) 322 [1407.6129].
- [85] Planck collaboration, Planck 2013 results. XXXI. Consistency of the Planck data, Astron. Astrophys. 571 (2014) A31 [1508.03375].
- [86] S. Yaser Ayazi and A. Mohamadnejad, Conformal vector dark matter and strongly first-order electroweak phase transition, JHEP 03 (2019) 181 [1901.04168].
- [87] S. Yaser Ayazi and A. Mohamadnejad, Scale-Invariant Two Component Dark Matter, Eur. Phys. J. C 79 (2019) 140 [1808.08706].

- [88] XENON collaboration, Dark Matter Search Results from a One Ton-Year Exposure of XENON1T, Phys. Rev. Lett. 121 (2018) 111302 [1805.12562].
- [89] LZ collaboration, First Dark Matter Search Results from the LUX-ZEPLIN (LZ) Experiment, 2207.03764.